Discontinuous Metal Thin Films & the Single Electron Transistor

***James E. Morris[1], C. Radehaus[2], M. Hietschold[2], A. Kiesow[2] and* F. Wu**

[1] Dept of Electrical & Computer Engineering, Portland State University, OR 97207-0751, USA, j.e.morris@ieee.org, [2] Chemnitz University of Technology, Germany, [3] Medtronic, Austin TX

Abstract

Traditional conduction models for island films on insulating substrates are based on electrostatically activated tunneling, but under-estimate actual conductances by orders of magnitude. A modified model has made significant headway with this problem, as demonstrated by simulations. Practical applications of discontinuous films are impeded, however, by the difficulty of fabricating reproducible, stable structures, particularly for low TCR films which are the most susceptible to drift. A technique to manufacture stable and reproducible films is described. The simplest discontinuous "film" is the single island coulomb block, which forms the basis of the single-electron transistor (SET). Room temperature SETs employ chains of islands, i.e. 1-D discontinuous films.

Keywords

Discontinuous metal films, single electron transistors, conduction, injection model

1 Introduction

1.1 Discontinuous thin metal films

Discontinuous thin metal films are readily formed in the early stages of nucleation and growth of noble or refractory metal films (Au, Ag, Pt, Pd, W, Mo) on insulating substrates, such as glass (e.g. soda-lime, Corning 7059), alumina, polymers (e.g. polyimides), or cleaved crystal surfaces, typically by physical vapor deposition *in vacuo*. Other processes may be used, the key element being a weak atom-substrate interaction. The films consist of discrete metal islands, of dimensions in the 2 – 10 nm range, separated by inter-island gaps of 2 nm or more. These parameters can vary considerably with the metal/substrate material system and deposition parameters, especially substrate temperature. Significant electronic conduction is observed in discontinuous films with island diameters and gaps in the 1 to 10 nm range [1-4]. Applications for these films might be strain gages, hydrogen sensors, IR-detectors, negative resistance switching devices, conductive wear coatings (polymerized) and electron emitters. The stability and reproducibility of these films are important for successful commercial development of any such applications.

1.2 Conventional Electronic Conduction Theory

The Boltzmann distribution relates the charged island density N to the total island density N_∞ by

$$N = N_\infty \exp - \delta E/kT .$$

The electrical conductance may be expressed as

$$\sigma = \sigma_0 \exp -\delta E/kT,$$

where

$$\delta E = (q^2/4\pi\varepsilon)\,(r^{-1}-(r+s)^{-1})$$

is the zero field electrostatic energy required to charge a small spherical island of radius, r, by removal of an electron to distance, s, (the inter-island separation,) in a medium of dielectric constant ε, q is the electronic charge, k is Boltzmann's constant, T is the absolute temperature, and

$$\sigma_0 = \lambda\,(4\pi m q^2/\,h^3 B).(\pi BkT / \sin \pi BkT).\exp - A\phi^{1/2}$$

is the electron tunneling term, with

$$B = \tfrac{1}{2}A\phi^{1/2}\ \&\ A = 4\pi s\,(2m)^{1/2}/\,h,$$

where h is Planck's constant, and λ, m, and ϕ are the effective tunneling area, electronic mass, and tunneling barrier height. Island size, r, increases with average film thickness, and hence δE decreases, (assuming constant deposition conditions.) By contrast, gap widths, s, tend to remain constant with thickness [2], due to a well-defined atomic capture distance around the islands.

2 Single Electron Transistors (Set)

In discontinuous film conduction theory, the energy required to charge an island as a prerequisite to charge transport is provided randomly by the film's thermal energy. At T = 0, there is no such energy source available, and the charging energy must be provided by the applied field itself. The Coulomb block system is the most basic form of discontinuous film, consisting of one single island (Fig. 1(a)), with the property shown in Fig. 1(b) that no current flows below the threshold, conventionally expressed as $qV \geq \delta E$ [5-8]. Clearly, the applied field, F, can similarly provide a portion of the island charging energies at finite temperatures, and this contribution is conventionally included in discontinuous film models by a field reduction of the electrostatic activation energy. In a treatment which exactly parallels Schottky effect theory [9, 10],

$$\delta E = (q^2/4\pi\varepsilon)\,(r^{-1}-(r+s)^{-1}) - (2r+s)qF$$

at low electric field

$$F < (q/4\pi\varepsilon)(r+s)^{-2},$$

and

$$\delta E = (q^2/4\pi\varepsilon)r^{-1} + (r/s)(2r+s)qF - 2(q^2/4\pi\varepsilon s)^{1/2}((2r+s)qF)^{1/2}$$

at high field.

$$\delta E \rightarrow 0 \text{ at } qV = (1 + s/r)\delta E_{V=0}\ ,$$

i.e. the threshold field is a little higher than usually quoted (Figure 1(b)). Already such devices have been fabricated for demonstration at low temperatures, and STMs or AFMs are increasingly being used as accurate nano-fabrication tools [11-13].

One of the most exciting recent developments in microelectronics has been the development of single electron logic devices [6 – 8,14 – 16] from the basic concept of the two terminals Coulomb blockade. The fundamental idea is that the charge can be placed on the island by a third, control electrode, permitting the flow of low voltage current (Figure 1(a)). The practical problem with the SET concept is to make the devices work at room temperature, or at least at T > 77 K. To do this, δE must be much greater than kT [15, 16], to some specified acceptable probability of random thermal charging, exp-(δE/kT), with the additional benefit that the Coulomb block threshold is also increased.. The obvious solution is to reduce island dimensions. A rough calculation for $\delta \sim 10kT$ at T = 300 K, shows that island dimensions of around 1 nm will be necessary taking this approach, i.e. smaller than those demonstrated to date [15]. An alternative approach is to increase $\delta E = q^2/2C$ by de-

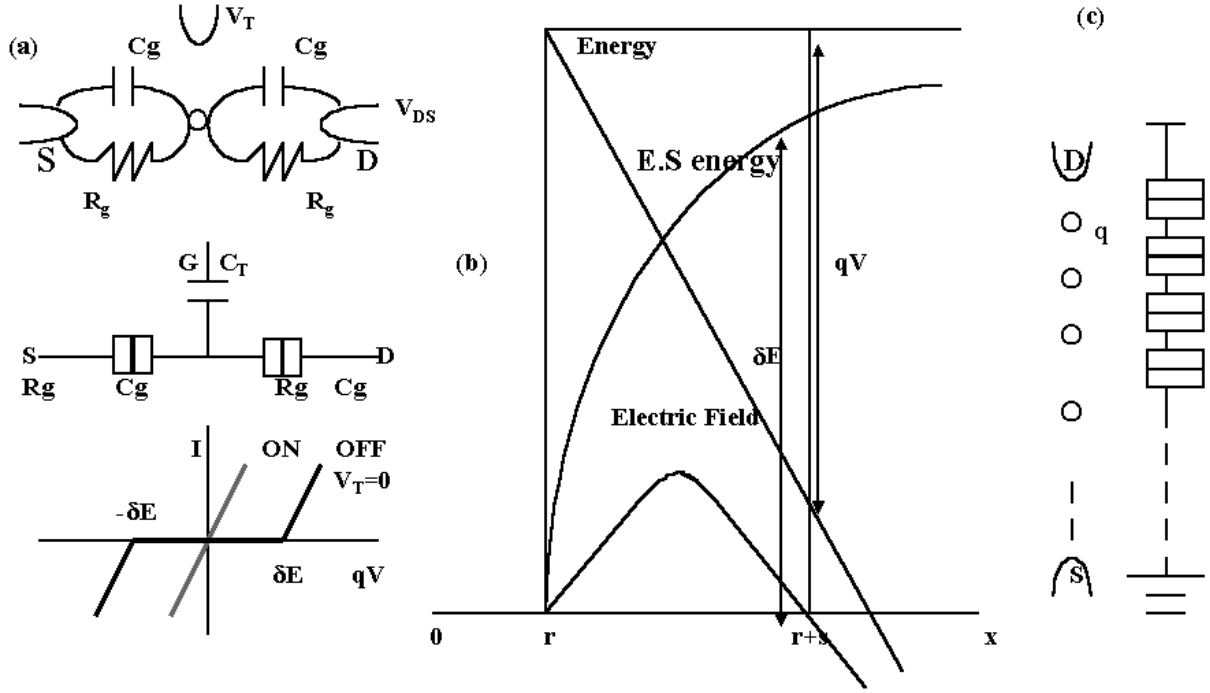

Figure 1: (a) Coulomb block system, consisting of one single island
(b) property of SET
(c) string of n islands

creasing system $C = C_g/n$ for a string of n islands (Figure 1(c)). One implementation of this concept [16] does not actually use discrete metal islands, but instead allows a percolation channel of nano-crystallites in a polycrystalline silicon film to define the "island" chain. In this case, n is an uncontrollable parameter, but if it is large enough, the fluctuations may be small. Nevertheless, it would be clearly preferable to be able to control the number, size, and position of a chain of metal islands for such devices, and this is a goal of the AFM deposition program described below.

3 AFM Fabrication

Scanning Tunneling Microscopy (STM) and/or Atomic Force Microscopy (AFM) technologies provide the means to control island positions. Various techniques have been proposed for applications in similar systems [17], predominantly on silicon, and follow earlier methods using the electron microscope to fabricate thin metal lines, arrays of metal dots, etc. The difference in the current goal of control of discontinuous film island placement is one of scale. Essentially any means of producing a physical change on the substrate to act as a subsequent nucleation site during deposition can work, e.g. electron polymerization of residual oil vapors to produce a localized carbon deposit. Or, taking advantage of the known preferential nucleation on negative charge sites [18] may be more successful if the charge sites can remain localized for a sufficient length of time. Certainly AFM indentation of soft substrates would be more permanent, but the technique is limited to polymers and may not work on glass or ceramic. If one applies sufficient field to the emission tip, atoms may be stripped from the end as in a field ion microscope. Film deposition by such a technique may be feasible, but is not expected to be practical. However, the properties of chromium as an adhesion promoter for noble metals on substrates such as glass is well known; if one can

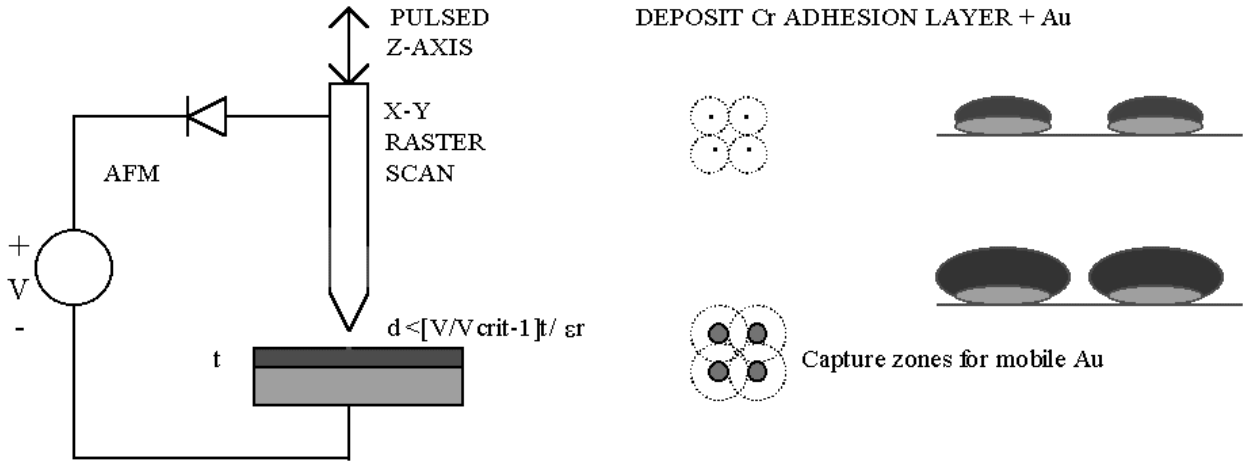

Figure 2: (a) AFM-piezo-electric drive system and (b) deposition model

establish small chromium nucleation sites to act as localized condensation centers in subsequent noble metal deposition, one may also achieve film stability along with reproducibility and structural regularity.

Some initial work has been performed along these lines [19]. A silicon AFM tip has been coated with chromium, and connected to an electrical source. The position of the tip above an insulating substrate (oxidized silicon for the purpose of the test) is controlled by the AFM/STM piezoelectric drive system. In the particular case in question, the probe height was kept constant and the applied voltage was pulsed, but it could be more convenient to apply a fixed potential and reduce the distance to the substrate to exceed the threshold field for emission of chromium atoms from the tip (Figure 2(a)). Chromium islands have been successfully deposited by the former technique, but much too large at 3 μm in diameter for the intended purpose. Work continues to reduce the chromium island dimensions by reducing the number of atoms deposited, by controlling the discharge current and time (Figure 2(a)).

A 10 nA current (e.g. defined by the diode reverse saturation current) for 10 ns (z-axis pulse) would ideally produce an approximately 3.5 nm diameter hemispherical island, or in practice one somewhat larger if the observation of about three atoms deposited per electron passed persists to low current levels, and more spread due to a substrate contact angle less than $\pi/2$ for strong adhesion. But seed islands of about this dimension on a regular grid would be very appropriate for subsequent deposition of gold or palladium for strain gauge or H_2 sensor applications. The overcoat deposition must be made at a temperature for which the island capture distance for ad-atoms exceeds half the gap between the chromium seed islands (Figure 2(b)). The chromium islands pin the noble metal islands to the designed location, and for thin overcoats or large seeds also define the island contact dimension (Figure 2(b), but in most cases small seeds or thicker overlays will be desired, to ensure control of the film property by the gold, palladium, etc., (Figure 2(b)). For most of the sensor applications, large islands with small gaps are required, whereas the SET emphasis is on small islands.

4 Discontinuous Thin Metal Films

4.1 Experimental Discrepancies

Borziak et al [20] reported three significant experiments. With previously deposited electrodes, they were able to fabricate discontinuous films with smaller islands and/or wider gaps immediately adjacent to the contacts. These symmetrical "inhomogeneous" films showed that the voltage drop is always greater at the positive end of the film. The second result was the observation of stable and reproducible switching in such films, but the explanation of this effect is a goal of future work, and will not be discussed further here. In the third experiment, the inhomogeneous films were also made asymmetric, i.e. with different inhomogeneous structures at the two electrodes, whereupon the dc resistance became polarity dependent; i.e. it displayed a diode-like effect. These results cannot be explained on the basis of existing conduction models, and indicate that the conduction mechanism must depend significantly upon the islands at the electrodes [21].

The asymmetric film study has been extended to AC effects [22]. In the traditional model, the film is regarded as a matrix of identical island/gap elements, with the metal island resistance in series with the parallel combination of gap tunnel resistance R_g and capacitance C_g, where

$$\delta E = \tfrac{1}{2} q^2 / C_g .$$

C_g values determined by AC measurements on this model are universally orders of magnitude greater than those consistent with δE. With the asymmetrical inhomogeneous film, two corner frequencies appear, yielding two distinct values for both R_g and C_g, corresponding to the two electrodes. In addition, the C_g values match

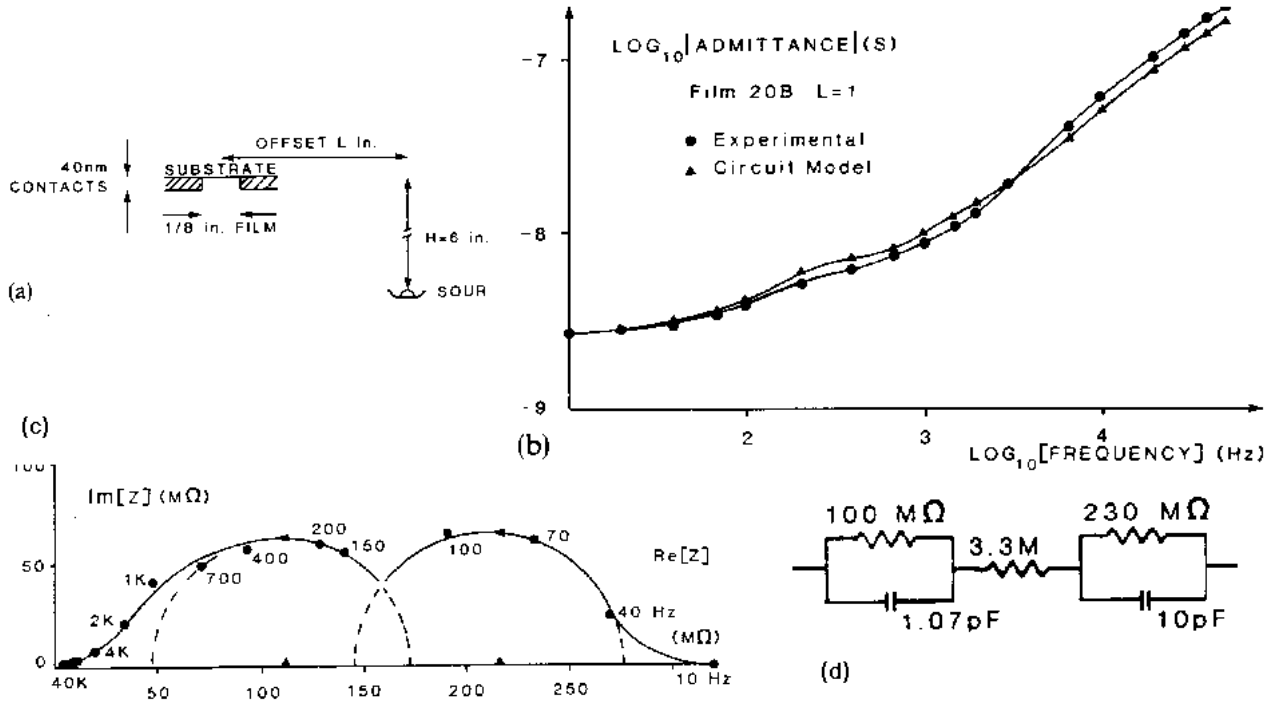

Figure 3: Asymmetrical AC-effects in discontinuous metal thin films.
(a) offset deposition source;
(b) admittance plot shows two corner frequencies;
(c) Cole plot verifies model
(d) of low d.c. film resistance with two contact RC elements

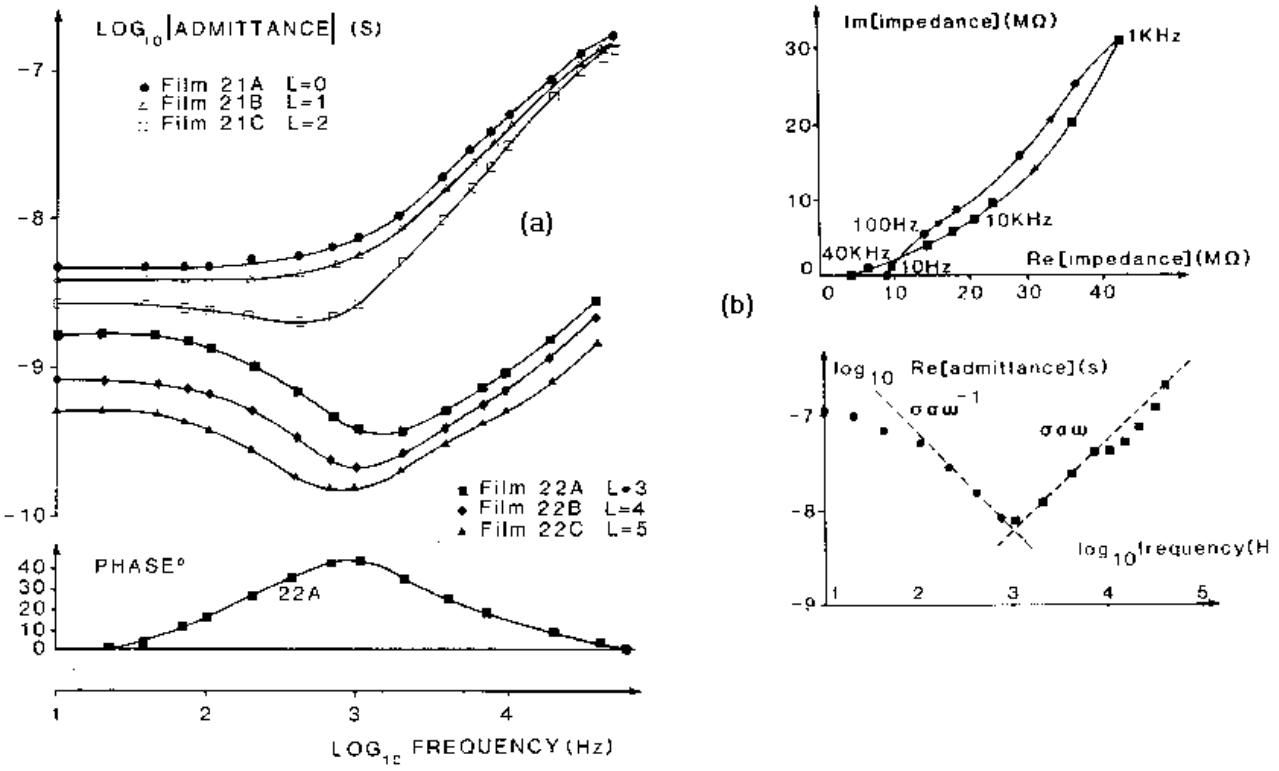

Figure 4: Extremely asymmetrical film demonstrating pseudo-inductance.
(a) Admittance/phase vs. frequency, and
(b) real and imaginary components plots.

well to capacitances between the electrodes and film across a single gap width. At extreme asymmetries, a "pseudo-inductive" effect makes an appearance, (as one contact resistance becomes very large,) representing a time delay to establish steady-state conductance in the film by charge carrier injection. Figures 3 and 4 show these effects.

5 New Conduction Model

5.1 Contact Injection Model

The results above lead to the concept of contact injection as the primary source of electrons and holes in the film, with the term "hole" referring to a positively charged island. With zero field, bulk charge separation occurs by tunneling between initially neutral islands, but immediate recombination will commonly follow. Eventually enough charges will drift apart to establish an equilibrium balance between generation and recombination, determined by the Boltzmann distribution. This is the traditional carrier density model, which predicts lower conductances than observed. When a voltage is applied to the film, these carriers will begin to drift in the field, and additional carriers will be injected at the electrodes. As the injected carriers drift into the center of the film, the film conductance rises after some time to the steady state value. This is the origin of the pseudo-inductive effect, with the applied field governing the rate of current rise.

The effects above apply to symmetrical film structures, whether homogeneous or inhomogeneous. If one adds the asymmetrical provision, then the different injection probabilities at the positive and negative electrodes produce the diode effect. The "diode" effect requires a quantitative difference in the electronic transfer probabilities at the positive and negative electro-

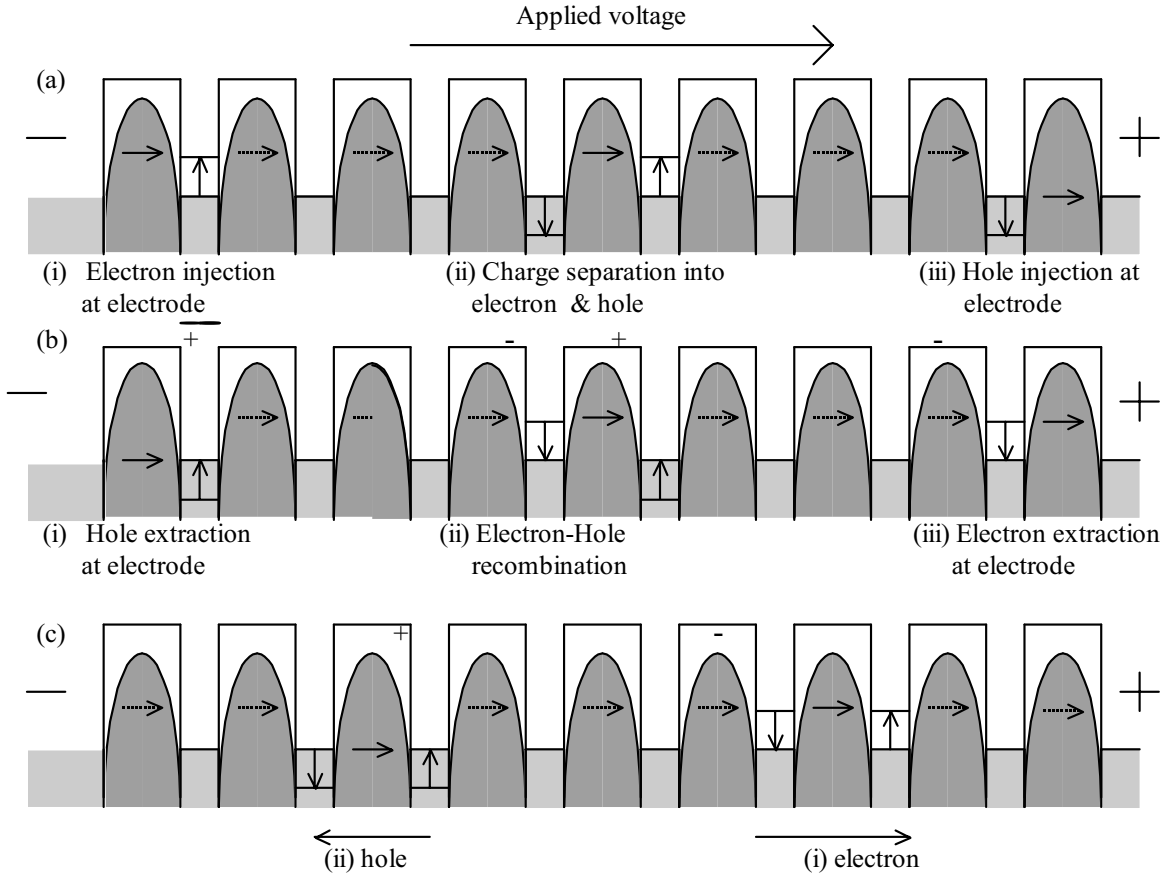

Figure 5: Energy diagrams for electron tunneling transfer modes:
(a) Charge injection (initially uncharged islands), (i) electron injection, (ii) charge separation, and (iii) "hole" injection;
(b) charge removal (initially charged islands), (i) "hole" removal, (ii) recombination, and (iii) electron removal; and
(c) charge transport in the central film (i) electron transfer, and (ii) "hole" transfer [23]. (The island charges shown refer to the initial states before electron transfer.)

des, a concept supported by the Borziak observation of a higher field at a positively biased electrode than when it is negatively biased [20]. The basis of the difference is shown in Figure 5, which illustrates energy diagrams for each of the six charge transfer mechanisms. In (a), the three charging processes shown apply to initially neutral islands, whereas in (b) the islands are initially charged, and are neutralized by the electron transfer, and (c) represents the charge "drift" mechanism which dominates transport across the film. In all cases zero field is assumed, and the "films" as shown are electrically neutral. The solid horizontal arrows represent the electron transfer, at the appropriate energy level, and the quadratic tunneling barriers shown include image charge effects. The shaded areas mark equilibrium Fermi levels, and the vertical arrows indicate the δE electrostatic energy level shifts from initial to final Fermi levels in the islands. Electrode Fermi levels are fixed. The electrostatically charge activated injection processes will be the limiting factors in charge transport, and it is immediately apparent that injection tunneling resistance at the negative electrode is less than that at the positive one. Current continuity will therefore require a higher field at the positive end, and the non-uniform field

implies that the film carries a net charge at equilibrium, which will require a finite time to become established.

The electrical behavior of a highly idealized discontinuous thin film has been modeled to verify the concepts developed above by demonstration of the experimental effects described [23]. The results presented below are for a 100 x 100 array of metal islands on a regular 6nm square grid. With the exception of the "anomalous" row of 1 nm islands 5 nm from the grounded electrode, all are 3 nm diameter islands separated by 3 nm gaps. The islands are assumed to be spherical for δE calculations, but cubic for the determination of tunneling areas, λ, in σ_0. T = 300 K, $\varepsilon_r = 2.5$, and $\phi = 1$ eV. The voltage across the film is $V_{appl} = 10^{-4}$ volts.

To establish initial conditions, the number of equilibrium charged islands is calculated from the Boltzmann distribution, and positive and negative values are assigned randomly in the array. At t = 0, voltage is applied and the initial field distribution determined iteratively for the random charge locations. Tunneling probabilities are calculated for all gaps along and across the film, and time is incremented. The probability calculations are repeated at each time increment, and a tunneling transition occurs whenever the accumulated probability exceeds 0.5. The charge separation and recombination processes are simplified: any adjacent positive and negative islands are assumed to immediately recombine, and the underlying Boltzmann distribution re-established by the random assignment of two charged islands elsewhere. Only the tunneling events in Figure 5 are considered, (i.e. there are no doubly charged islands,) and there is no

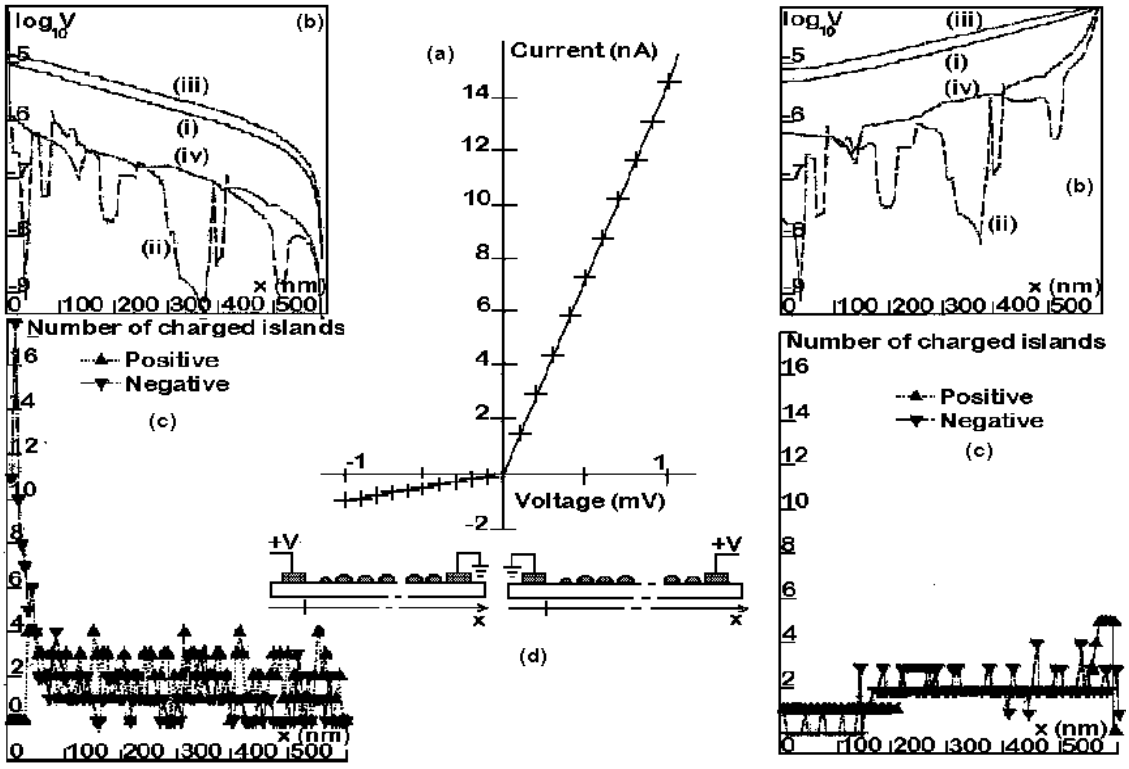

Figure 6: (a) Diode effect, with superimposed
(b) potential and
(c) charge distributions along the film, with negative and positive biases as defined in schematics (d) [23].
(Note position of small island, large gap at left-hand end of film.)

activation energy associated with the transitions in (b) and (c) where the total system electrostatic energy is unchanged, (i.e. the reduced δE postulated for this case, due to the difference between static and high frequency values of ε [24], is set to zero.)

5.2 Simulation results

The diode effect shown in Figure 6(a) matches the form of Borziak's observation [20], even to the roughly 10:1 conductance ratio. Superimposed on the I-V characteristic in Figure 6 are (b) the (log) potential distributions and (c) the charge distributions along the film for negative and positive applied voltages, as defined in the schematics (d). Both field distributions also compare favorably with the general experimental forms (which is more obvious in a linear format). Four separate potential plots along the film are shown for each bias in Figure 6: (i) the average potential across the film, and the potentials along three individual island columns. There are 100 columns along the film, so (ii) column 2 is one in from one edge, (iii) column 98 is two in from the opposite edge, and (iv) column 50 is in the middle. The greater field curvatures (and fluctuations) along the edges correspond to greater charged island densities than in the middle (due to mutual repulsion between like charges.) It is expected that the systematic study of field and charge distributions at higher applied fields will yield a discontinuity and the reproducible switching effect observed in inhomogeneous films. Figure 7 shows the "turn-on" transient, which demonstrates both the pseudo-inductive effect, and the ratio of final to initial currents. The initial conductance corresponds to the traditional theoretical value based on the equilibrium Boltzmann charge density.

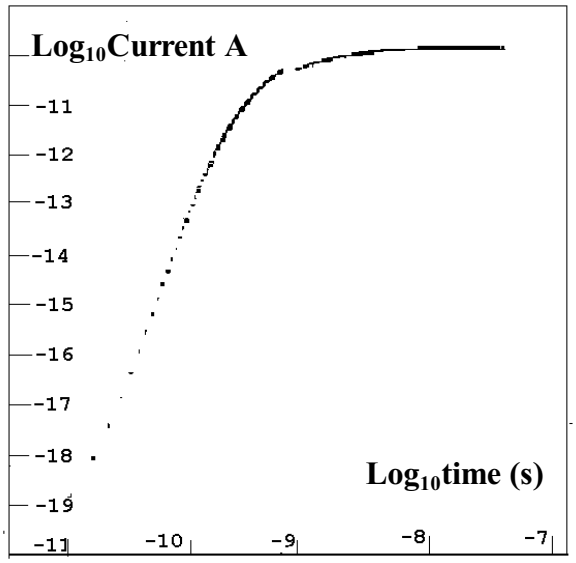

Figure 7: Transient current response [23]

6 Conclusions

The consistent observation of larger conductances in discontinuous thin films than traditional models predict has been explained by a contact injection model [23], which also accounts for the diode effect in asymmetric films, and for anomalous AC results, including pseudo-inductance. (An alternate theoretical approach to the diode effect does not explain the AC observations [25]. Renewed interest in sensor applications of discontinuous films is expected to follow the demonstration of structural stability in ion-plated strain gauges [26]. A greater level of structural control is made possible by AFM technology, with both reproducibility and stability achievable. Current research is under way to apply this concept to the fabrication of room temperature SETs. [27,28) The discontinuous thin film model is also being applied to the SET, especially to the chain structure, in order to understand the device operation more completely [29]. Switching effects have been observed for some time, but reproducible switching only recently [30]. Future applications will incorporate sensing or switching effects with the SET structure.

References

1. C.A. Neugebauer in *Handbook of Thin Film Technology*, L.I. Maissel & R. Glang, editors, (McGraw-Hill) 1970.
2. L.L. Kazmerski & D.M. Racine, *Journal of Applied Physics*, 46 (1975) 791.
3. J.E. Morris & T.J. Coutts, *Thin Solid Films*, 47 (1977) 3 – 65.
4. R.M. Hill, *Proc. of the Royal Society, London, Series A*, 309 (1969) 397.
5. D.V. Averin & K.K. Likharev, *J. Low Temp. Physics*, 62 (1986) 354.
6. J.R. Tucker, *J. Appl. Phys*., 72 (1992) 4399.
7. D.K. Ferry, J.B. Barker & C. Jacoboni, editors, *Granular Nanoelectronics*, Plenum, (1991).
8. H. Ahmed & K. Nakazato, *Microelectronic Engineering*, 32 (1996) 297.
9. L.A. Weitzenkamp & L.M. Bashara, *Transactions Metallurgical Society AIME*, 236, (1966) 351.
10. J.E. Morris, *Thin Solid Films*, 11, (1972) 81 – 89.
11. K. Matsumoto, *Proc. IEEE*, 85 (4), (1997) 612 – 628.
12. J. Servat, P. Gorastiza, F. Sanz, F. Perez-Murano, N. Barniol, G. Abagal & X. Aymerich, *J. Vac. Sci. Technol A.* 14 (3) (1996) 1208 – 1212.
13. F. Perez-Murano, G. Abagal, N. Barniol, X. Aymerich, J. Servat, P. Gorastiza & F. Sanz, *J. Appl. Physics*, 78 (1995) 6797 – 6801.
14 K. Nakazato, R.J. Blaikie, J.R.A. Cleaver & H. Ahmed, *Electronics Lett*.,.29 (4), (1993) 384.
15. W. Rosner, F. Hofmann, T. Vogelsang & L. Risch, *Microelectronic Engineering* 27 (1995) 55 – 58.
16. K. Yano, T. Ishii, T. Hashimoto, T. Kobayashi, F. Marai, & K. Seki, *IEEE Trans. Electron Devices*, 41 (1994) 1628.
17. H. Pagnia, *5th Int. Workshop Elec. Props. Metal/Non-Metal Microsyst*., Polanica, 1995.
18. J.E. Morris, *Metallography*, 5, (1972) 41 – 58.
19. F. Mueller, M. Hietschold & J.E. Morris, ZfM, Technische Universität Chemnitz-Zwickau, 1996.
20. P. Borziak, V. Diukov, A. Kostenko, Yu. Kulyupin & S. Nepijko, *Thin Solid Films*, 36, (1976) 21.
21. J.E. Morris, A. Mello & C.J. Adkins, in *Physical Phenomena in Granular Materials*, D. Cody, T.H. Geballe & P. Sheng, editors, Materials Research Society Proceedings 195, 181 – 186, MRS, Pittsburgh, 1990.
22. J.E. Morris, *Thin Solid Films*, 193/194, (1990) 110 – 116.
23. J.E. Morris & F. Wu, *10th International Conference on Thin Films*, Salamanca, Sept., 1996; *Thin Solid Films*, 317 (1998) 178 – 182.
24. K.D. Leaver, *J.Phys.C*, 10, (1977) 249.
25. R.D. Federovich, A.G. Naumovets & P.M. Tomchuk, *Physics Reports*, 328 (2000) 73 – 179.
26. J.E. Morris, A. Kiesow, M. Hong & F. Wu, *5th Int. Workshop Elec. Props. Metal/Non-Metal Microsyst.*, Polanica, 1995; *Int. J. Electronics*, 81(4), (1996) 441 – 447.
27. J.E. Morris, *"Single Electron Transistors"*, in *"Electrical Engineering Handbook,"* R. Dorf (ed) CRC Press (3rd edition) 2004 (in press.)
28. J.E. Morris F. Wu, C. Radehaus, M. Hietschold, A. Henning, K. Hofmann, & A. Kiesow, (Invited) *7th Internat. Conf. Solid State & Integrated Circuit Technology (ICSICT), Beijing,* 19 – 21 Oct, 2004.
29. J.E. Morris, *6th Int. Workshop Elec. Props. Metal/Non-Metal Microsyst.*, Prague, 1997; *Vacuum*, 5 (1998) 107 – 113.
30. A. Kiesow, J.E.Morris, C. Radehaus, & A. Heilmann, *J. Appl. Phys*. 94 (2003) pp. 6988 – 6990.